Interplay of strong chemical bonds and the repulsive Coulomb force in the metastable states of triply ionized homonuclear molecules: A theoretical study of N_2^{3+} and O_2^{3+}

Yutaka Imamura[1,*] and Takaki Hatsui[2]

[1]*Department of Chemistry and Biochemistry, School of Advanced Science and Engineering, Waseda University, Tokyo 169-8555, Japan*

[2]*RIKEN SPring-8 Center, 1-1-1 Kouto, Sayo-cho, Sayo-gun, Hyogo 679-5148, Japan*

(Received 25 September 2011; published 31 January 2012)

We have studied metastable electronic states of trication molecules for N_2^{3+} and O_2^{3+} using the internally contracted multireference configuration interaction method with single and double excitations (icMRCISD). The metastable ground state for O_2^{3+} and metastable excited state for N_2^{3+} were obtained with the barriers of approximately 1.5 and 13.0 kcal/mol, respectively, although those metastable states were not found in previous calculations. The analysis on occupation numbers of natural orbitals demonstrates that the two metastable states are formed owing to the balance between the reduction of cationic Coulomb repulsion and the weakening of the chemical bonds. We have proposed to measure these metastable states by short-wavelength free-electron lasers (sFELs) that have the potential to produce excited states of multiply charged molecules.

DOI: 10.1103/PhysRevA.85.012524 PACS number(s): 31.15.vn, 31.15.A−

I. INTRODUCTION

Recent advances in free-electron laser (FEL) technologies have enabled the production of laser pulses strong enough to fully ionize molecules in the short-wavelength regime [1]. A single photon with sufficiently short wavelength can ionize valence electrons as well as inner valence and core electrons. Multiple photoionization by short-wavelength FEL (sFEL) then produces molecules with holes in any orbitals, i.e., excited states of the multiply ionized molecules. sFEL thus provides an opportunity to investigate the excited states of multiply ionized molecules such as ionized states with multiple holes in inner-valence orbitals, which have been practically impossible or extremely difficult to produce experimentally. The photoionization mechanism and produced species are investigated experimentally by the FEL intensity dependence of ion charge distribution [2], and momenta of the ions [3–5]. These experiments, however, do not provide detailed information for specifying the ground and excited electronic states of multiply charged atoms or molecules as the intermediates in the multiple photoionization processes. In this paper we have studied theoretically the potential curves of multiply charged molecules in order to obtain knowledge regarding the metastable states.

Trications of diatomic molecules are generally seldom encountered because of the instability caused by the confined positive charge. However, several have been examined theoretically and experimentally [6–13]. The experimentally observed species are as follows: diatomic halogens [5,6], SF^{3+} [8], B_2^{3+} [9], Mo_2^{3+} [10], Se_2^{3+} [11], Te_2^{3+} [11], and LaF^{3+} [11]. Except for the SF^{3+}, these were reported by using mass spectrometry. This is in accordance with the fact that all these species have a lifetime longer than microsecond order. On the other hand, theoretical approach focused on Coulomb explosion rather than the characters of ground and excited states for trication molecules [12,13] although doubly ionized states were recently examined in terms of relaxations [14,15]. Metastable states of homonuclear diatomic molecules containing nitrogen and oxygen atoms have never been reported experimentally and theoretically. This study explores the possibility of metastable ground and excited states for N_2^{3+} and O_2^{3+} using the internally contracted multireference configuration interaction method with single and double excitations (icMRCISD) [16,17].

II. RESULTS AND DISCUSSIONS

The potential curves of five lowest N_2^{3+} and O_2^{3+} states for each symmetry of A_g, B_{1g}, B_{2g}, B_{3g}, A_u, B_{1u}, B_{2u}, and B_{3u} in D_{2h}, which was reduced from the original $D_{\infty h}$ symmetry, were investigated by icMRCISD calculations using the correlation-consistent polarized valence quintuple-zeta (cc-pV5Z) basis set [18]. The spin multiplicity was set to 2. The configuration spaces consisting of eight orbitals including $2s\sigma$, $2s\sigma^*$, $2p\sigma$, $2p\pi$, and $2p\pi^*$ type orbitals were optimized by complete active space self-consistent-field (CASSCF) calculations with equal weights for the participating states of the same spin multiplicity in D_{2h} symmetry. The single and double excitations from CASSCF reference states were considered. All icMRCISD calculations were carried out by the MOLPRO program [19].

First, let us examine O_2^{3+}. We have calculated O_2^{3+} 48 potential curves with eight symmetries, calculated at the icMRCISD level with cc-pV5Z. The potential curves are drawn in Supplemental Materials [20]. All curves except one metastable state are repulsive and tend to converge to three curves at the O-O distance more than 2.2 Å. The metastable state has A_g symmetry and a rather shallow minimum with a barrier height ∼1.5 kcal/mol, which makes experimental detection of this state difficult owing to its very short lifetime. The O-O bond distance of the potential minimum is estimated to be around 1.2 Å, which is close to the equilibrium distance of the neutral molecule and suggests that the O-O bond is not stretched compared with the neutral ground state.

In order to investigate the metastable state in more detail, the three lowest states with A_g symmetry at $R = 1.2$ Å are selected and analyzed by natural orbital analysis (Fig. 1). The

*imamura@kurenai.waseda.jp

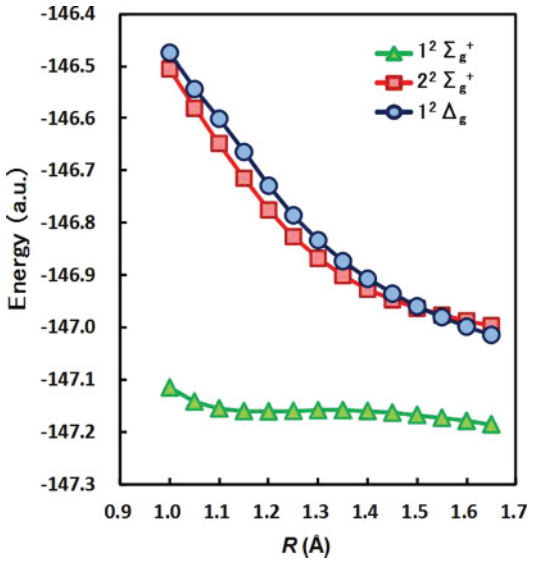

FIG. 1. (Color online) O_2^{3+} potential curves of three states with A_g symmetry in D_{2h}, calculated at the icMRCISD level with the cc-pV5Z basis set.

first and second lowest states, which correspond to Σ_g^+ states in $D_{\infty h}$, are labeled as $1\ ^2\Sigma_g^+$ and $2\ ^2\Sigma_g^+$. The third state with $^2\Delta_g$ symmetry in $D_{\infty h}$ is labeled as $1\ ^2\Delta_g$. First, we study the electronic states around the equilibrium distance of the neutral molecule. Table I lists occupation numbers of natural orbitals of $2s\sigma$, $2s\sigma^*$, $2p\sigma$, $2p\pi$, and $2p\pi^*$ for O_2^{3+} with the O-O bond distance 1.2 Å. The occupation numbers of $2s\sigma$, $2s\sigma^*$, and $2p\sigma$ exhibit slight variations among three states: 1.96–1.98, 1.85–1.90, and 1.03–1.09, respectively. The main difference between first and second (third) states is the occupation numbers of $2p\pi$ and $2p\pi^*$: 1.79 and 1.09 (1.04) for $2p\pi$; 0.21 and 0.90 (0.95) for $2p\pi^*$. This comparison indicates that the lowest state $1\ ^2\Sigma_g^+$ has more electrons in $2p\pi$ than in $2p\pi^*$, whereas the $2\ ^2\Sigma_g^+$ and $1\ ^2\Delta_g$ states have electrons in $2p\pi^*$ comparable to those in $2p\pi$. Thus, the $2\ ^2\Sigma_g^+$ and $1\ ^2\Delta_g$ states are less stable than the $1\ ^2\Sigma_g^+$ state.

Next, we explore the reason for the appearance of the metastable state by analyzing the bond-distance dependence of the occupation numbers of four orbitals from the highest occupied molecular orbital (HOMO), namely, $2s\sigma^*$, $2p\sigma$, $2p\pi$, and $2p\pi^*$. The occupation numbers with the distance from 1.1 to 1.5 Å are listed in Table II. The $2p\pi$ and $2p\pi^*$ occupation numbers are also plotted in Fig. 2. The solid and dotted lines correspond to $2p\pi$ and $2p\pi^*$, respectively. Note that the occupation numbers of $2s\sigma$ are more than 1.93 and do not play an important role in the formation of the metastable state. As the O-O bond is elongated, the occupation numbers of $2s\sigma^*$ and $2p\sigma$ hardly change, especially for the O-O distance

TABLE I. Natural occupation numbers of O_2^{3+} with $R = 1.2$ Å

State	$2s\sigma$	$2s\sigma^*$	$2p\sigma$	$2p\pi$	$2p\pi^*$
$1\ ^2\Sigma_g^+$	1.97	1.90	1.03	1.79	0.21
$2\ ^2\Sigma_g^+$	1.96	1.85	1.09	1.09	0.90
$1\ ^2\Delta_g$	1.98	1.85	1.08	1.04	0.95

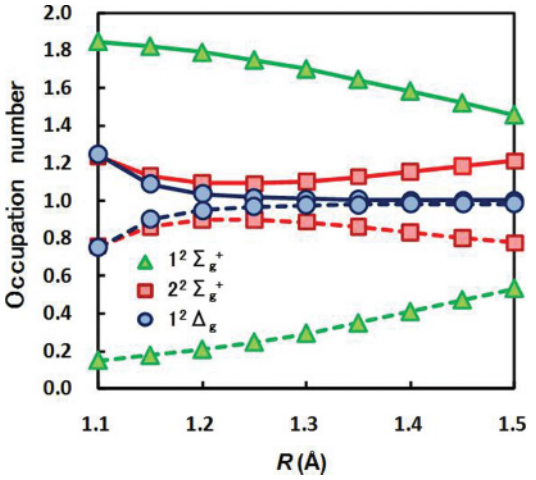

FIG. 2. (Color online) Natural occupation numbers of $2p\pi$ and $2p\pi^*$ for O_2^{3+} at the distance from 1.1 to 1.5 Å. The solid and dotted lines correspond to $2p\pi$ and $2p\pi^*$, respectively.

from 1.25 to 1.5 Å. Thus, these two orbitals are not essential for the metastable state.

Let us examine the remaining $2p\pi$ and $2p\pi^*$ orbitals. As illustrated in Fig. 2, the occupation number of $2p\pi$ monotonically decreases and that of $2p\pi^*$ monotonically increases for $1\ ^2\Sigma_g^+$ as the O-O bond distance increases. On the other hand, the $2\ ^2\Sigma_g^+$ and $1\ ^2\Delta_g$ states exhibit a mixed behavior: The occupation number of $2p\pi$ ($2p\pi^*$) decreases (increases) with $R = 1.1$–1.25 Å for $2\ ^2\Sigma_g^+$ and $1\ ^2\Delta_g$, increases (decreases) for $2\ ^2\Sigma_g^+$, and scarcely changes for $1\ ^2\Delta_g$ with $R = 1.25$–1.5 Å. Note that the $2p\pi$ and $2p\pi^*$ orbitals are doubly degenerate, and the changes of the occupation numbers as shown in Table II and Fig. 2 should be doubled. This analysis demonstrates that the elongation of the O-O bond induces electron transfer from $2p\pi$ to $2p\pi^*$, which leads to instability in terms of chemical bond although

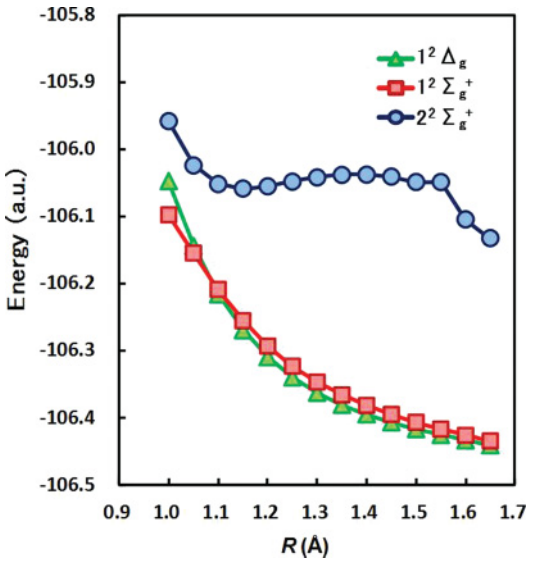

FIG. 3. (Color online) N_2^{3+} potential curves of three states with A_g symmetry in D_{2h}, calculated at the icMRCISD level with the cc-pV5Z basis set.

TABLE II. Natural occupation numbers of O_2^{3+} with distances R ranging from 1.1 to 1.5 Å.

	$2s\sigma^*$			$2p\sigma$			$2p\pi$			$2p\pi^*$		
R (Å)	$1\,^2\Sigma_g^+$	$2\,^2\Sigma_g^+$	$1\,^2\Delta_g$	$1\,^2\Sigma_g^+$	$2\,^2\Sigma_g^+$	$1\,^2\Delta_g$	$1\,^2\Sigma_g^+$	$2\,^2\Sigma_g^+$	$1\,^2\Delta_g$	$1\,^2\Sigma_g^+$	$2\,^2\Sigma_g^+$	$1^2\Delta_g$
1.10	1.90	1.58	1.45	1.04	1.39	1.48	1.85	1.23	1.25	0.15	0.76	0.75
1.15	1.90	1.77	1.75	1.04	1.18	1.19	1.82	1.13	1.09	0.18	0.86	0.90
1.20	1.90	1.85	1.85	1.03	1.09	1.08	1.79	1.09	1.04	0.21	0.90	0.95
1.25	1.91	1.89	1.89	1.02	1.04	1.04	1.75	1.09	1.02	0.25	0.90	0.97
1.30	1.91	1.90	1.91	1.02	1.02	1.02	1.70	1.10	1.01	0.29	0.89	0.98
1.35	1.91	1.91	1.92	1.01	1.01	1.01	1.65	1.13	1.01	0.35	0.86	0.98
1.40	1.91	1.92	1.92	1.00	1.00	1.00	1.58	1.16	1.00	0.41	0.83	0.98
1.45	1.92	1.93	1.93	0.99	0.99	0.99	1.52	1.19	1.00	0.47	0.80	0.98
1.50	1.92	1.93	1.93	0.99	0.98	0.99	1.46	1.21	1.00	0.53	0.78	0.99

the Coulomb repulsion of positive charges decreases. Thus, the appearance of the metastable state is ascribed to the fact that weakening of the chemical bond outweighs the stability from the reduction of Coulomb repulsion.

Secondly, let us examine N_2^{3+}. We have calculated N_2^{3+} 56 potential curves with eight symmetries, calculated at the icMRCISD level with cc-pV5Z. The potential curves are drawn in Supplemental Material [20]. All curves except one curve are repulsive. Although the metastable state of O_2^{3+} is a ground state, that of N_2^{3+} is an excited state with Σ_g^+ symmetry and provides a barrier height of ~13.0 kcal/mol, which may permit us to observe experimentally. The barriers are reproduced in all the calculations with a wide variety of basis sets and different active space, or relativistic effects. See the details in the Appendix. The N-N bond distance of the metastable state is estimated to be around 1.15 Å, which is close to that of O_2^{3+}.

The three lowest states at $R = 1.2$ Å as shown in Fig. 3 are analyzed using a procedure similar to the one used for O_2^{3+}. The first lowest state with $^2\Delta_g$ symmetry in $D_{\infty h}$, is labeled as $1\,^2\Delta_g$. The second and third lowest states, which correspond to Σ_g^+ states in $D_{\infty h}$, are labeled as $1\,^2\Sigma_g^+$ and $2\,^2\Sigma_g^+$. Table III lists occupation numbers of natural orbitals of $2s\sigma$, $2s\sigma^*$, $2p\sigma$, $2p\pi$, and $2p\pi^*$ for N_2^{3+} with the N-N bond distance 1.2 Å. Although the occupation numbers of $2s\sigma$ do not change significantly even for N_2^{3+}, the $2s\sigma^*$ occupation numbers strongly depend on the states: The occupation numbers for $1\,^2\Delta_g$ and $1\,^2\Sigma_g^+$ are 1.87 and 1.76, whereas that of $2\,^2\Sigma_g^+$ is 0.44, which leads to the instability of $2\,^2\Sigma_g^+$ and makes $2\,^2\Sigma_g^+$ an excited state. The occupation number of $2p\sigma$ for $2\,^2\Sigma_g^+$ is smaller than those of the other states by approximately 0.25. The $2p\pi$ and $2p\pi^*$ natural orbitals are more occupied for $2\,^2\Sigma_g^+$ than for the other two states. This tendency about $2p\pi$ is also confirmed for the metastable state of O_2^{3+}.

TABLE III. Natural occupation numbers of N_2^{3+} with $R = 1.2$ Å.

State	$2s\sigma$	$2s\sigma^*$	$2p\sigma$	$2p\pi$	$2p\pi^*$
$1\,^2\Delta_g$	1.97	1.87	1.02	0.95	0.09
$1\,^2\Sigma_g^+$	1.96	1.76	1.00	1.01	0.09
$2\,^2\Sigma_g^+$	1.89	0.44	0.76	1.69	0.24

Next, we investigate the metastable state of N_2^{3+} by analyzing the bond-distance dependence of the occupation numbers of $2s\sigma^*$, $2p\sigma$, $2p\pi$, and $2p\pi^*$ for the three lowest states. The occupation numbers with the distance R from 1.1 to 1.5 Å are listed in Table IV. The $2p\pi$ and $2p\pi^*$ occupation numbers are also plotted in Fig. 4. The behaviors of the occupation numbers for N_2^{3+} seem more complicated than those for O_2^{3+}. The $2s\sigma^*$ occupation number of the $2\,^2\Sigma_g^+$ state increases with $R = 1.2$–1.4 Å and then jumps into 1.64 at $R = 1.45$ Å. On the other hand, those of $1\,^2\Delta_g$ and $1\,^2\Sigma_g^+$ (quasi-)monotonically approach ~1.88. The $2p\sigma$ occupation number of the $2\,^2\Sigma_g^+$ state decreases with the N-N distance with $R = 1.2$–1.4 Å and then jumps into 1.15 at $R = 1.45$ Å in a similar way. On the other hand, those of $1\,^2\Delta_g$ and $1\,^2\Sigma_g^+$ are approximately 1.0 and exhibit a significantly small bond-distance dependence.

Let us discuss $2p\pi$ and $2p\pi^*$ orbitals. Figure 4 demonstrates that the N-N bond elongation decreases the occupation numbers of $2p\pi$ for $1\,^2\Sigma_g^+$ and $2\,^2\Sigma_g^+$ and slightly decreases those of $1\,^2\Delta_g$ for $R < 1.45$ Å as is observed in O_2^{3+}. The opposite trend is also observed for $2p\pi^*$; namely, the N-N bond elongation increases the occupation numbers of $2p\pi^*$ for $2\,^2\Sigma_g^+$ and those of $1\,^2\Sigma_g^+$ and $1\,^2\Delta_g$ slightly increases.

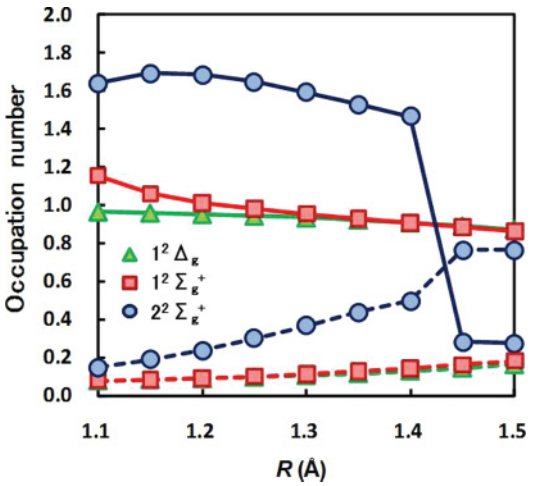

FIG. 4. (Color online) Natural occupation numbers of $2p\pi$ and $2p\pi^*$ for N_2^{3+} at the distance from 1.1 to 1.5 Å. The solid and dotted lines correspond to $2p\pi$ and $2p\pi^*$, respectively.

TABLE IV. Natural occupation numbers of N_2^{3+} with distances R ranging from 1.1 to 1.5 Å.

	$2s\sigma^*$			$2p\sigma$			$2p\pi$			$2p\pi^*$		
R (Å)	$1\,^2\Delta_g$	$1\,^2\Sigma_g^+$	$2\,^2\Sigma_g^+$	$1\,^2\Delta_g$	$1\,^2\Sigma_g^+$	$2\,^2\Sigma_g^+$	$1\,^2\Delta_g$	$1\,^2\Sigma_g^+$	$2\,^2\Sigma_g^+$	$1\,^2\Delta_g$	$1\,^2\Sigma_g^+$	$2\,^2\Sigma_g^+$
1.10	1.87	1.53	0.56	1.01	0.99	0.88	0.97	1.16	1.64	0.08	0.08	0.15
1.15	1.87	1.69	0.44	1.02	1.00	0.82	0.96	1.06	1.69	0.08	0.08	0.19
1.20	1.87	1.76	0.44	1.02	1.00	0.76	0.95	1.01	1.69	0.09	0.09	0.24
1.25	1.87	1.80	0.51	1.01	1.00	0.68	0.94	0.98	1.65	0.09	0.10	0.30
1.30	1.87	1.83	0.62	1.01	1.00	0.59	0.93	0.95	1.59	0.10	0.11	0.37
1.35	1.87	1.84	0.74	1.01	1.00	0.49	0.92	0.93	1.53	0.12	0.13	0.44
1.40	1.87	1.85	0.87	1.00	1.00	0.42	0.91	0.91	1.46	0.13	0.14	0.50
1.45	1.88	1.86	1.64	1.00	1.00	1.15	0.89	0.89	0.28	0.14	0.16	0.76
1.50	1.88	1.87	1.69	0.99	0.99	1.08	0.87	0.86	0.28	0.16	0.18	0.77

For $R \geqslant 1.45$ Å, the occupation numbers of $2p\pi$ and $2p\pi^*$ for $2\,^2\Sigma_g^+$ are approximately 0.28 and 0.77, which destablize the $2\,^2\Sigma_g^+$ state. The above analysis on the $2\,^2\Sigma_g^+$ state reveals that the significant electron transfer of $\{2p\pi, 2p\sigma\} \rightarrow \{2s\sigma^*, 2p\pi^*\}$ plays a crucial role in the appearance of the metastable state.

Lastly, we discuss the possibility of detecting the excited metastable state of N_2^{3+}. The excited bound state found in this paper, however, has a shallow potential strongly mixed with dissociation channels, which suggests that its state cannot be observed by a conventional spectroscopy such as mass spectrometry because of its short lifetime. In this paper, we propose to detect its state by using photoelectron spectroscopy of bound N_2^{2+}. The bound nature of the $2\,^2\Sigma_g^+$ state can be traced by a sharper photoelectron feature due to its potential curve parallel to that of the ground state of N_2^{2+} in the Franck-Condon region as depicted schematically in Fig. 5.

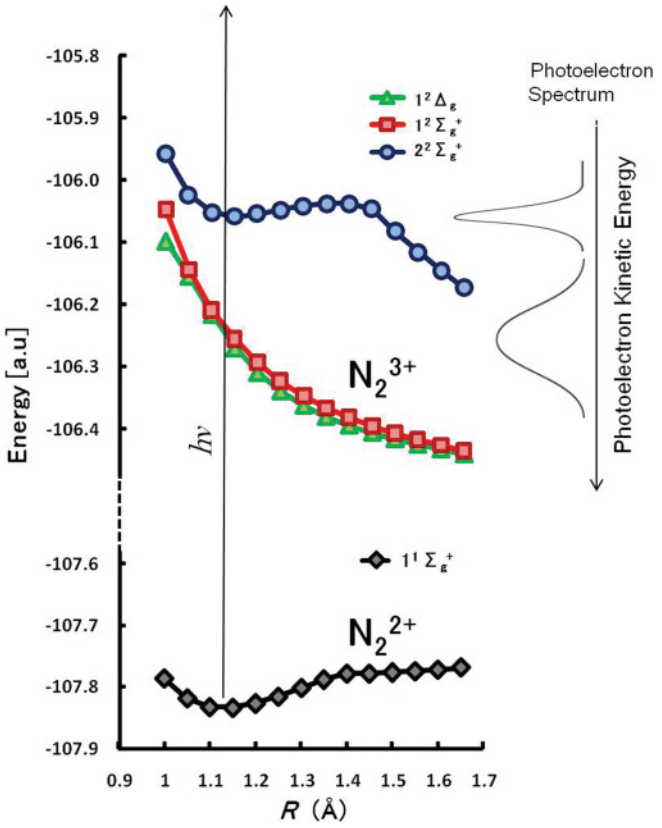

FIG. 5. (Color online) Schematic potential curves of N_2^{2+} and N_2^{3+}.

The feasible experimental scheme is as follows: (I) N_2^{2+} is generated by two-photon ionization with sFEL [21–23] due to its high peak intensity. (II) The third photon then ionizes it to N_2^{3+} by the delayed sFEL pulse. By using second- or third-harmonic sFEL with double or triple photon energy, the photoelectron features associated with process (II) have higher kinetic energy than those from process (I). The two processes are therefore well separated in the kinetic energy space. The spectrum from process (II) will still be complex because the target sharp photoelectron line associated with the $2\,^2\Sigma_g^+$ state overlaps the background photoelectrons produced by ionization of dissociative N_2^{2+}. The time delay between processes (I) and (II) provides N_2^{2+} time to dissociate resulting that the background feature becomes simple photoelectron lines from the dissociated nitrogen atoms. It will be possible, therefore, to observe the $2\,^2\Sigma_g^+$ state experimentally with advanced photoelectron spectroscopy with FEL producing photons in the energy higher than the energy difference between the ground state of N_2^{2+} and the metastable state, i.e., approximately 50 eV. From the viewpoint of the photoelectron

TABLE V. Barriers of $2\,^2\Sigma_g^+$ for N_2^{3+} in kcal/mol.

Basis set	Active space	Barrier
Nonrelativistic calculation		
cc-pVTZ	Valence	9.7
aug-cc-pVTZ	Valence	9.8
cc-pVQZ	Valence	12.1
aug-cc-pVQZ	Valence	12.2
aug-cc-pVQZ	Valence+Rydberg1	12.2
aug-cc-pVQZ	Valence+Rydberg2	12.2
cc-pV5Z	Valence	13.0
cc-pCV5Z	Valence	13.0
cc-pV5Z+DH Rdyberg	Valence	13.0
cc-pV5Z+DH Rdyberg	Valence+Rydberg1	13.0
cc-pV5Z+DH Rdyberg	Valence+Rydberg2	13.0
Relativistic calculation		
cc-pV5Z-DK	Valence	12.7

cross section, the extreme ultraviolet regime around 60–100 eV is the most suited for this study.

Recently, coincidence spectroscopy of Auger electron has been reported to provide information on dissociative HBr^{3+} potential energy curves and reveals the remaining binding energy in the Franck-Condon region [24]. This spectroscopy is also applicable to detect the bound $N_2{}^{3+}$ state if its photoelectron feature is successfully distinguished from other decay channels.

III. CONCLUSION

The icMRCISD study reveals that the two metastable states of $N_2{}^{3+}$ and $O_2{}^{3+}$ are excited and ground states, respectively. This difference originates in the generation of holes in deep orbitals for $N_2{}^{3+}$. The analysis on occupation numbers of natural orbitals reveals that the detailed balance between Coulomb repulsion and chemical bond is the key to forming metastable states. Their bond distances, which are about 1.2 Å close to the neutral equilibrium ones, is consistent with the bond length region where the remarkable weakening of strong chemical bonds occurs along with the bond elongation.

This study focuses on homonuclear diatomic molecules $N_2{}^{3+}$ and $O_2{}^{3+}$. However, a similar metastable state may be formed for heteronuclear diatomic molecules such as CO and NO molecules. Research along this line is in progress. The spin multiplicity was limited to 2 in this study, but high spin states can be generated because multiphotoionization by sFELs or other experimental methodologies do not have strict spin selection rules. The comparison with high spin states will give further insight into the character of the metastable states.

ACKNOWLEDGMENTS

We are grateful for kind support from Professor Hiromi Nakai, and thank Dr. Mitsuru Nagasono for the discussion on the sFEL experiments. This paper is a part of the outcome of research performed under Waseda University Grants for Special Research Projects (Project No. 2009B-163). We are also grateful to Global Center of Excellence (COE) "Practical Chemical Wisdom" from MEXT, Japan.

APPENDIX

We evaluate barriers of the $2\,^2\Sigma_g{}^+$ state for $N_2{}^{3+}$ changing basis sets and active spaces with or without relativistic effects. Table V shows barriers calculated at the icMRCISD level with the correlation-consistent polarized (cc-p) basis sets of {cc-pVTZ [triple zeta (TZ)], cc-pVQZ [quadruple zeta (QZ)], cc-pV5Z (quintuple zeta)} and its augmented versions of {aug-cc-pVTZ, aug-cc-pVQZ, and aug-cc-pV5Z} in the nonrelativistic scheme. The scalar second-order Douglas-Kroll (DK)-Hess approach [25,26] is also adopted for relativistic calculations with cc-pV5Z-DK [12,27], Single (s, p) Rydberg basis functions of Dunning-Hay are added for describing ($3s$, $3p$) orbitals [28]. Three types of active spaces are examined: Valence space including three A_g, one B_{2g}, one B_{3g}, three B_{1u}, one B_{2u}, and one B_{3u} orbitals; valence space+one more B_{1u} orbital, named as Rydberg1; valence space+B_{2u} and B_{3u} orbitals named as Rydberg2. Note that the barriers are estimated by changing bond lengths from 1.0 to 1.6 Å with an interval of 0.5 Å. Although the small energy differences between (aug-)cc-pVTZ and the other higher basis sets are observed, the barriers are estimated to be 12–13 kcal/mol for the higher basis sets. The relativistic effects and selections of the active spaces do not significantly vary barriers.

[1] L. Young *et al.*, Nature **466**, 56 (2010).
[2] A. A. Sorokin, S. V. Bobashev, T. Feigl, K. Tiedtke, H. Wabnitz, and M. Richter, Phys. Rev. Lett. **99**, 213002 (2007).
[3] R. Moshammer *et al.*, Phys. Rev. Lett. **98**, 203001 (2007).
[4] A. Rudenko *et al.*, Phys. Rev. Lett. **101**, 073003 (2008).
[5] G. Zhu, M. Schuricke, J. Steinmann, J. Albrecht, J. Ullrich, I. Ben-Itzhak, T. J. M. Zouros, J. Colgan, M. S. Pindzola, and A. Dorn, Phys. Rev. Lett. **103**, 103008 (2009).
[6] R. J. Verver, J. S. Wright, and M. Y. Ivanov, J. Chem. Phys. **117**, 6991 (2002).
[7] H. Sakai, H. Stapelfeldt, E. Constant, M. Y. Ivanov, D. R. Matusek, J. S. Wright, and P. B. Corkum, Phys. Rev. Lett. **81**, 2217 (1998).
[8] K. Nagesha, V. R. Marathe, and D. Mathur, Chem. Phys. **154**, 125 (1991).
[9] D. L. Weathers, F. D. McDaniel, S. Matteson, J. L. Duggan, J. M. Anthony, and M. A. Douglas, Nucl. Instrum. Methods Phys. Res. B **56–57**, 889, (1991).
[10] T. T. Tsong, *Atom-Probe Field Ion Microscopy: Field Ion Emission, and Surfaces and Interfaces at Atomic Resolution* (Cambridge University Press, Cambridge, 2005).
[11] K. Franzreb, J. Hrušák, M. E. Alikhani, J. Lörinčík, R. C. Sobers, and P. Williams, J. Chem. Phys. **121**, 12293 (2004).
[12] G. Handke, F. T. Tarantelli, and L. S. Cederbaum, Phys. Rev. Lett. **76**, 896 (1996).
[13] A. D. Bandrauk, D. G. Musaev, and K. Morokuma, Phys. Rev. A **59**, 4309 (1999).
[14] J. H. D. Eland, M. Tashiro, P. Linusson, M. Ehara, K. Ueda, and R. Feifel, Phys. Rev. Lett. **105**, 213005 (2010).
[15] M. Tashiro, M. Ehara, H. Fukuzawa, K. Ueda, C. Buth, N. Kryzhevoi, and L. S. Cederbaum, J. Chem. Phys. **132**, 184302 (2010).
[16] H.-J. Werner and P. J. Knowles, J. Chem. Phys. **89**, 5803 (1988).
[17] P. J. Knowles and H.-J. Werner, Chem Phys. Lett. **145**, 514 (1988).
[18] T. H. Dunning Jr., J. Chem. Phys. **90**, 1007 (1989).
[19] MOLPRO, version 2010.1, a package of *ab initio* programs, H.-J. Werner, [http://www.molpro.net].
[20] See Supplemental Material at http://link.aps.org/supplemental/10.1103/PhysRevA.85.012524 for potential curves of $O_2{}^{3+}$ and $N_2{}^{3+}$.
[21] W. Ackermann *et al.* Nat. Photonics **1**, 336 (2007).
[22] T. Shintake *et al.*, Nat. Photonics **2**, 555 (2008).

[23] M. Cornacchia *et al.*, J. Synchrotron Radiat. **11**, 227 (2004).
[24] F. Penent, P. Lablanquie, J. Palaudoux, L. Andric, G. Gamblin, Y. Hikosaka, K. Ito, and S. Carniato, Phys Rev. Lett. **106**, 103002 (2011).
[25] M. Douglas and N. M. Kroll, Ann. Phys. (NY) **82**, 89 (1974).
[26] B. A. Hess, Phys. Rev. A **33**, 3742 (1986).
[27] W. A. de Jong, R. J. Harrison, and D. A. Dixon, J. Chem. Phys. **114**, 48 (2001).
[28] T. H. Dunning and P. J. Hay, in *Methods of Electronic Structure Theory*, edited by H. F. Schaefer III (Plenum, New York, 1977), Vol. 3.